SCIENCE CHINA
Earth Sciences

• RESEARCH PAPER •

October 2015 Vol.58 No.10: 1827–1839
doi: 10.1007/s11430-015-5104-8

# Statistical downscaling model for late-winter rainfall over Southwest China

RUAN ChengQing[1,2], LI JianPing[3,4*] & FENG Juan[3,4]

[1] *State Key Laboratory of Numerical Modeling for Atmospheric Sciences and Geophysical Fluid Dynamics, Institute of Atmospheric Physics, Chinese Academy of Sciences, Beijing 100029, China;*
[2] *College of Earth Sciences, University of Chinese Academy of Sciences, Beijing 100049, China;*
[3] *College of Global Change and Earth System Science, Beijing Normal University, Beijing 100875, China;*
[4] *Joint Center for Global Change Studies, Beijing 100875, China*

Received February 3, 2015; accepted March 20, 2015; published online May 15, 2015

A statistical downscaling model is built for the late-winter rainfall over Southwest China (SWC). A partial-correlation method is used for selecting factors. The results show that the selected factors for late-winter rainfall in SWC are sea level pressure in Western Europe (SNAO) and sea surface temperature in Western Pacific (WPT). SNAO is related to the southern pole of North Atlantic Oscillation (NAO) and excites Southern Eurasian teleconnection, which influences the development of the southern branch trough and the water vapor transport to SWC. WPT indicates the variability of ENSO in the tropical Western Pacific. WPT excites Pacific-East Asia teleconnection and an anticyclone (cyclone) is formed in the southern part of China and suppresses (enhances) rainfall over SWC. A regression statistical downscaling model using SNAO and WPT shows good performance in fitting the variability of late-winter rainfall in the whole SWC region and every observation station, and the model also shows strong robustness in the independent validation. The statistical model can be used for downscaling output from seasonal forecast numerical models and improve the SWC late winter rainfall prediction in the future.

**statistical downscaling, Southwest China, late-winter rainfall, partial correlation**

**Citation:** Ruan C Q, Li J P, Feng J. 2015. Statistical downscaling model for late-winter rainfall over Southwest China. Science China: Earth Sciences, 58: 1827−1839, doi: 10.1007/s11430-015-5104-8

Southwest China (SWC) is based on the Yunnan-Guizhou Plateau, and the autumn and winter rainfall in this region recently are shown to have undergone significant interdecadal changes and suffer more droughts (Liu et al., 2011; Zhang et al., 2011, 2013a, 2014; Gu et al., 2014; Yu et al., 2014). Especially for the year of 2009/2010, a severe drought with record extent started in the autumn and ended in the winter. More than 25 million residents suffered drinking-water shortage, and more than 1 million ha of crops died (Barriopedro et al., 2012; Zhang et al., 2012; Huang et al., 2012; Xu et al., 2012).

Many researchers have studied the external forcing factors that influence the autumn and winter rainfall over SWC, and these studies focus on the signals from the low or mid-high latitude regions. For low latitude factors, researchers analyze the tropical sea surface temperature over different regions and their influence on SWC rainfall (Huang et al., 2012; Feng et al., 2014). Some studies emphasize that the SWC drought in 2009/2010 occurred under the background of decadal aridification over the southern China, which is related to the increasing CP El Niño events in recent decades (Zhang et al., 2011, 2014); Zhang et al. (2013b) also pointed out that the 2009 CP El Niño event was character-

*Corresponding author (email: ljp@bnu.edu.cn)

ized by the relatively farther westward location and the strongest intensity among all the CP El Niño events in the past 60 years, which was the main reason causing the severe drought over SWC in the autumn of 2009. For the mid-high latitude factors, Song et al. (2011) indicated the winter North Atlantic Oscillation (NAO) can produce the quasi-stationary waves propagating along the Asia-Africa subtropical jet and influence the winter rainfall over SWC. Xu et al. (2012) further stressed the asymmetric relationship between the winter NAO and SWC precipitation. In the positive NAO phase, the excited stationary waves are further northward and cannot propagate to SWC. So only the negative NAO phase can produce the stationary waves to induce the negative anomalous SWC winter rainfall. Yang et al. (2012) pointed out that the occurrence of the 2009/2010 drought over SWC is related to the anomalies of the atmospheric circulation systems in the westerly belt.

The projection results from the CMIP5 models show that the droughts over SWC will be further frequent in the future (Wang et al., 2014). Previous studies made detailed and thorough analysises of the extenal forcing factors to SWC rainfall, but few studies are focused on the prediction models. Rainfall prediction can provide estimates for economic governance strategy, so prediction model studies have great significance and realistic value. Besides, the importance of winter precipitation gets more attention recently. More winter rainfall causes cryogenic freezing rain and snow disaster whereas less rainfall causes severe droght (Tao et al., 2014). So it is meaningful for the study of winter rainfall over SWC. Because most of the SWC winter rainfall (70%) occurs between January and February, this paper analyzes SWC late-winter rainfall and builds the statistiacal downscaling model, which can help improve the prediction skill of late-winter SWC rainfall in the future.

Downscaling is a common method for studying local climate. In statistical downscaling method, the model is built between large scale circulation forcing factors and local rainfall, then the circulation prediction results from climate models are taken in the statistical model to get the local rainfall prediction in the future (Salathé, 2003; Hewitson and Grane, 2006; Fowler et al., 2007). Because the numerical climate models show better skill in simulating large scale circulation fields than local rainfall (Wilby, 1997; Yarnal et al., 2001), the statistical downscaling method can improve the ability of predicting local rainfall for climate models. Guo et al. (2011) took the 500 hPa geopotential height and the 700 hPa vapor transport as predictors and built the statistical downscaling model for the summer rainfall over the middle-lower reaches of the Yangtze River; Li et al. (2009) linked the principal modes of seansonal mean sea level presure (SLP) and winter rainfall over southern Australia, and built statistical downscaling for future projection; Guo et al. (2012) analyzed summer rainfall over North China using time-scale decomposition method and builtthe interannual and interdecadal rainfall models respectively, which effectively predicted the summer rainfall in the following years (Li et al., 2013a; Guo et al., 2014).

The method for forcing factor selection is important for the skill of statistical downscaling models. Stepwise regression method is widely used in previous studies, but this method can only explain limited variance and the selected factors will interfere with the next factor selection. Therefore, this paper proposes a partial-correlation method for selecting factors. In the partial-correlation method, the factors are selected based on the variance which is not explained by the old factors, so explained variance of models is improved. This paper uses the partial-correlation method to find the forcing factors influencing the SWC winter rainfall and builds the statistical downscaling model.

## 1 Data and methods

### 1.1 Data sources and Southwest China rainfall index

Observed rainfall data were derived from 160-station-monthly rainfall dataset for China provided by the China Meteorological Administration for the period of 1951–2014. We also used monthly China land rainfall dataset (V2.0) on a 0.5°×0.5° grid during 1961–2010. This dataset is used for empirical orthogonal function analysis over southern China.

The primary monthly data for atmospheric fields were extracted from the National Centres for Environmental Prediction-National Center for Atmospheric Research (NCEP-NCAR) reanalysis on a 2.5°×2.5° grid with 17 levels (Kalnay et al., 1996); monthly sea surface temperature (SST) data used in this study were taken from Hadley Centre SST Dataset I on a 1°×1° grid (Rayner et al., 2003). Several well-known climateindices are employed like northern annular mode (NAM) index (Li and Wang, 2003b), NAO index (Li et al., 2003a, 2013b), and ENSO-related indices (Niño1+2, Niño3, Niño3.4 and Niño4, http://www.cpc.noaa.gov/data/indices). All the data are the average of January and February for each year.

The region of SWC is based on the EOF analysis of late-winter rainfall over the southern China. The result indicates that all the southern China shows the same signal in the first mode (Figure 1(a)), and the variance center is located in South China. The second mode reveals distinct an east-west dipole (Figure 1(b)). The western pole includes the southwest of Yunnan, southern Sichuan, most Guizhou and western Guangxi; the other is located over Jiangxi, Zhejiang, and Fujian. The two regions show opposite signals. The EOF results indicate that the rainfall over SWC is one of the main variance centers in the late-winter rainfall in the southern China. So the regions of SWC is defined as 97.5°E–107.5°E, 21.5°N–27.5°N and there are 14 stations in this regions (Baise, Zunyi, Guiyang, Bijie, Xingren, Xichang, Huili, Lijiang, Dali, Baoshan, Kunming, Lincang, Mengzi and Jinghong). The averaged late-winter rainfall of the 14 stations is defined as Southwest China rainfall index

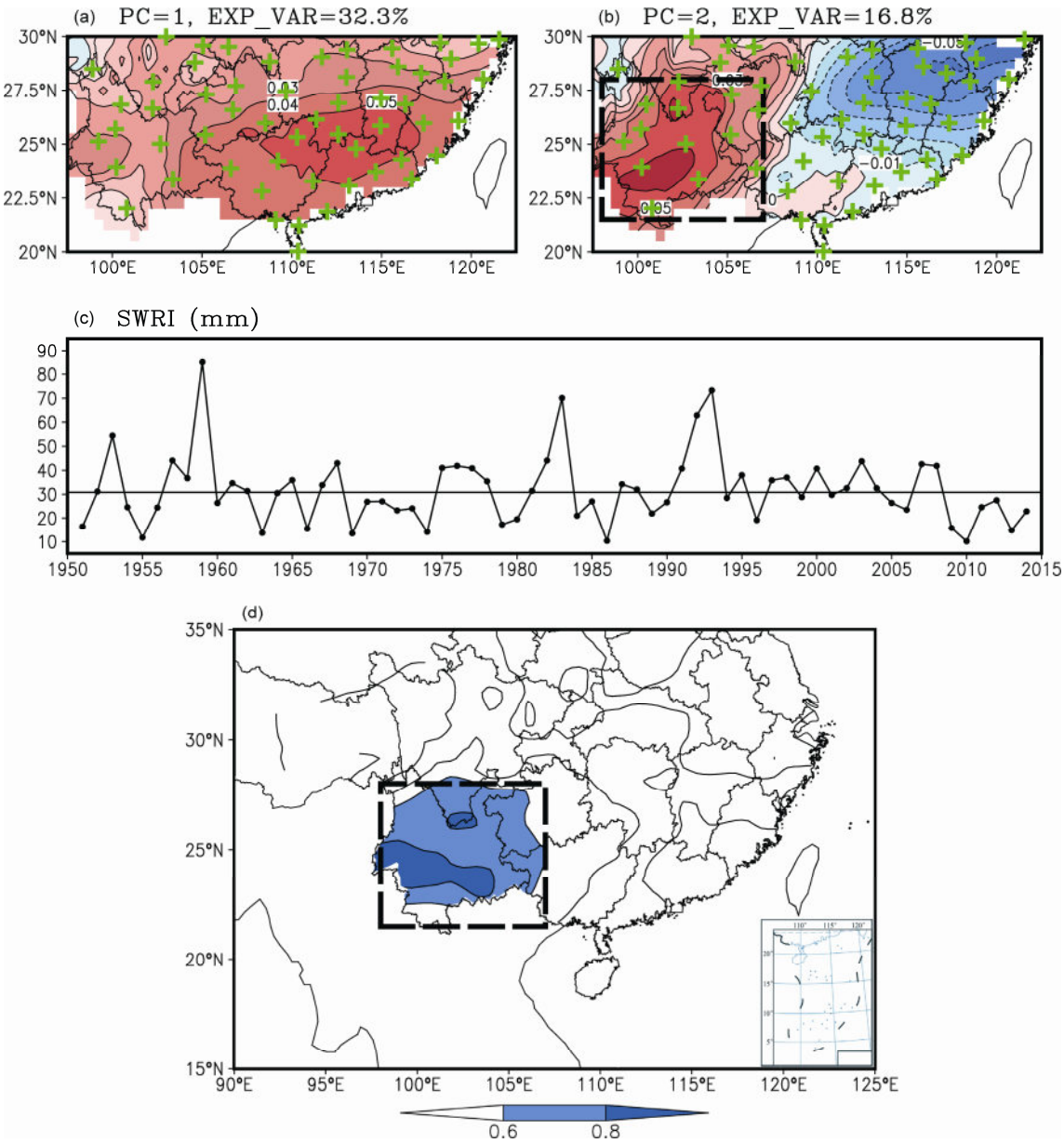


**Figure 1** The analysis of the late-winter rainfall over the southern China. (a) Spatial distribution of the first leading EOF mode of the late-winter southern China rainfall; the dashed box indicates Southwest China region used in this study (97.5°–107.5°E, 21.5°–27.5°N). The green crosses indicate the distribution of 160 gauge stations; (b) same as (a), but for the second leading mode; (c) the time series of Southwest China rainfall index, the straight line is the long-term mean (1951–2014). Unit: mm; (d) correlation map of late winter rainfall between SWRI and 160 gauge stations. The contour interval is 0.2.

(SWRI, Figure 1(c)) and SWRI shows good consistency with the rainfall over SWC (Figure 1(d)). Late-winter SWRI has significant interannual variance and a decreasing trend in the recent two decades. In the last six years (2009–2014), the values of SWRI are lower than the climate mean and the value of 2009/2010 is the least one since the year of 1950/1951.

### 1.2 Partial-correlation method for factor selection

Local rainfall is usually controlled by several external forcing factors. When the primary factor is found, this factor can only explain part of the rainfall variance. In order to find other factors related to the unexplained variance, this paper proposes the partial-correlation method. The main steps are: (1) identifying potential forcing factors with correlation analysis; (2) calculating root-mean-square errors (RMSE) for each of the potential factors with the leave-one-out cross validation method (Guo et al., 2011; Li et al., 2013a) and selecting the factor with the minimum RMSE; (3) testing the significance of the selected factor; (4) if the factor passes the significant test, removing the signal of this factor from the rainfall series and repeating Steps (1)–(3) with the left rainfall series to find the next forcing factor; if

the factor cannot pass the test, the selection is over.

The advantage of the partial-correlation method is that the new forcing factors are closely related to the unexplained rainfall variance and supplement the skill of old forcing factors. With more new factors selected, the explained variance gradually increases and the performance of the statistical model is improved (Figure 2). But the partial-correlation method is based on linear analysis, whereas some climate forcing has a nonlinear effect (Zhang et al., 2011, 2014, 2015). For example, the two types of ENSO warm events have opposite influences on the autumn rainfall over South China (Zhang et al., 2013b, 2015). Therefore, the partial-correlation method may be invalidated for the nonlinear climate forcing factors.

After the factor selection, the statistical model is build using local rainfall and factors. Although local rainfall has the nonlinear character, linear models show good performance on seasonal time scale. Besides, linear models are also widely used because of their simplicity and explicit physical meaning (Zorita and Storch, 1999; Guo et al., 2011, 2012). So, the linear regression method is applied to building the statistical downscaling model.

The assumption of statistical downscaling is that the relationship between local rainfall and forcing factors is stable. But in the long time scale, the interdecadal change of climate system may induce the change of statistical relationship. So after the model is built, an independent validation must be performed using observed data which are different from the model building period. In this paper, the data from 1951 to 1980 (30 yr) are used for training the model and the data from 1981 to 2014 (34 yr) are used for independent validation to test the robustness of the statistical downscaling model.

## 2 Selecting the factors for SWRI

Previous studies show that the remote forcing factors can influence local rainfall by teleconnection effect (Wilby and Wigley, 2000; Guo et al., 2012). So, the correlation is analyzed between SWRI and global circulation fields (geopotential height, SLP and SST) to find potential factors. The results are shown in Figure 3. There are several significant correlated regions in the pressure fields. One quasi-barotropic structure with a positive correlation with SWRI is located over the western Europe from the surface to the upper levels. A negative correlated region is located to the northeast of the quasi-barotropic structure on the lower levels. Over the east coast of North America, there is a dipole structure between the subtropical and mid-high latitude in Figure 3(b)–(d). Besides, some scattered significant correlation regions can be found on the 850 hPa geopotential height and SLP fields. There are only two main regions with a significant correlation in the SST field. The negative one is located in the tropical Western Pacific Ocean and the other positive one is located in the west coast of subtropical North America. All these significant correlated regions are the potential forcing factors that may influence the late-winter rainfall over SWC.

The boxes in Figure 3 are the regions of potential factors and the factor indices are defined as the areal mean of grids whose correlation coefficients are significant at the 95% confidence level. There are totally 22 potential factors in Figure 3 and RMSEs are calculated using leave-one-out cross validation method (Table 1). The forcing factor located in the SLP field over the western Europe (17.5°W–32.5°E, 22.5°–55°N) has the minimum RMSE and the correlation coefficient with SWRI (0.64) passes the significant test, so this is the first factor selected for the late-winter SWRI statistical model. This factor is named as SNAO (Southern pole of NAO) as it is located at the southern pole of winter NAO (Li and Wang, 2003a).

After the first factor is selected, the signal of SNAO is removed from SWRI according to partial-correlation method:

$$\begin{aligned}\mathrm{SWRI}_1 &= \mathrm{SWRI} - \mathrm{SWRI}_{\mathrm{SNAO}} \\ &= \mathrm{SWRI} - 4122.8 - 4.09 \times \mathrm{SNAO},\end{aligned}$$

the unit of $\mathrm{SWRI}_1$, SWRI and $\mathrm{SWRI}_{\mathrm{SNAO}}$ is mm, and the unit of SNAO is hPa. $\mathrm{SWRI}_1$ is linearly independent with SNAO, so the variance of $\mathrm{SWRI}_1$ cannot be explained by SNAO. The correlation is calculated between $\mathrm{SWRI}_1$ and circulation fields to find the next forcing factor (Figure 4).

One important character in Figure 4 is that the significant correlated regions located over western Europe and the eastern coast of North America in Figure 3 now cannot not be found. This result implies these factors have the same forcing effect as SNAO. Since the factor of SNAO is already selected, these factors are not necessary for the model. Besides, some factors still can be found in Figure 4 and their areas get larger, like the factors in the SLP field over the tropical Atlantic; some new factors are identified this time, like the factors in the upper levels of geopotential height

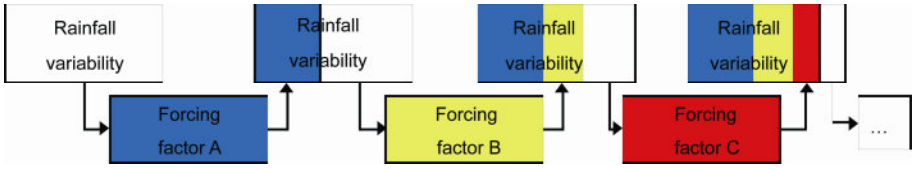


**Figure 2** Schematic graph for partial-correlation based factor selection method. White indicates unexplained rainfall variability. Different colors indicate different factors and explained rainfall variability. Each factor is selected based on the unexplained part (white) of rainfall variability.

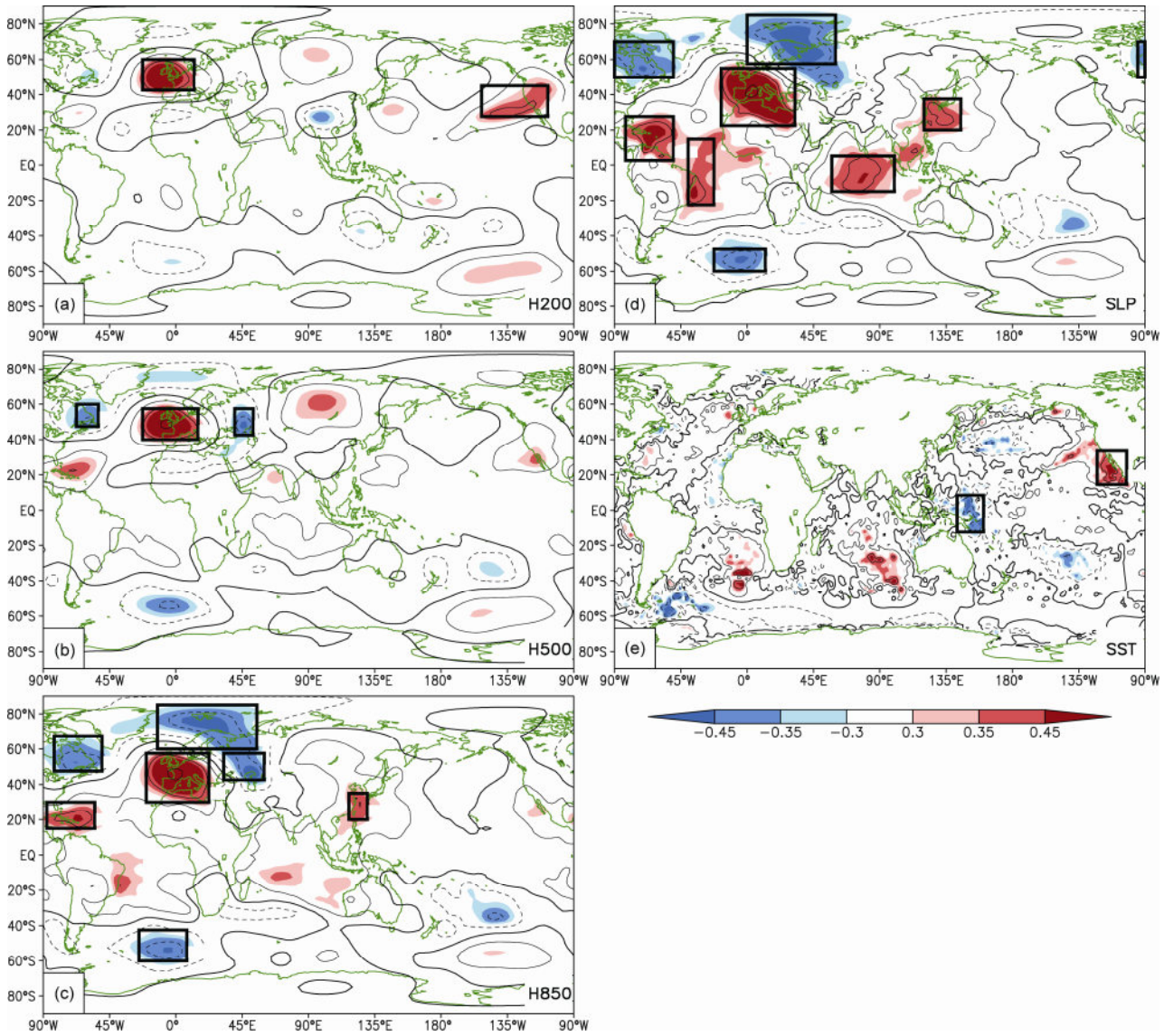


**Figure 3** Correlation maps between late-winter SWRI and (a) 200 hPa geopotential height, (b) 500 hPa geopotential height, (c) 850 hPa geopotential height, (d) SLP and (e) SST during 1951–1980. The boxes are the regions of potential factors. The contour interval is 0.2. The shaded areas indicate statistically significant correlation at the 90%, 95%, and 99% confidence levels respectively.

**Table 1** The four potential factors with the minimum RMSE during the cross validation in Steps (1)–(3) of factor selection (1951–1980)

| | Potential factors | Longitude | | Latitude | | $R$ [a)] | RMSE |
|---|---|---|---|---|---|---|---|
| Step 1 | SLP (Western Europe) | 17.5°W | 32.5°E | 22.5°N | 55°N | 0.64** | 12.4 |
| | H850 (Western Europe) | 20°W | 22.5°E | 30°N | 57.5°N | 0.64** | 12.5 |
| | H500 (Western Europe) | 22.5°W | 15°E | 40°N | 57.5°N | 0.61** | 12.8 |
| | H200 (Western Europe) | 22.5°W | 12.5°E | 42.5°N | 60°N | 0.56** | 13.4 |
| Step 2 (Remove SNAO) | SST (tropical Western Pacific) | 139.5°E | 159.5°E | 13.5°S | 14.5°N | −0.50** | 10.8 |
| | SST (Tropical Atlantic) | 34.5°W | 2.5°E | 11.5°S | 4.5°N | −0.15 | 11.0 |
| | H850 (Southern Pacific) | 162.5°W | 132.5°W | 35°S | 17.5°S | −0.35* | 11.3 |
| | SLP (South Atlantic) | 42.5°W | 20°W | 32.5°S | 0 | 0.39* | 11.4 |
| Step 3 (Remove SNAO and WPT) | H200 (Northern Pacific) | 62.5°E | 80°W | 52.5°N | 87.5°N | 0.15 | 8.5 |
| | H850 (Northern Pacific) | 125°E | 80°W | 55°N | 85°N | 0.02 | 8.7 |
| | H200 (Eastern China) | 92.5°E | 130°E | 22.5°N | 42.5°N | −0.12 | 8.7 |
| | H500 (Northern Pacific) | 115°E | 87.5°W | 52.5°N | 85°N | 0.13 | 8.9 |

a) * Significant at the 95% level; ** significant at the 99% level.

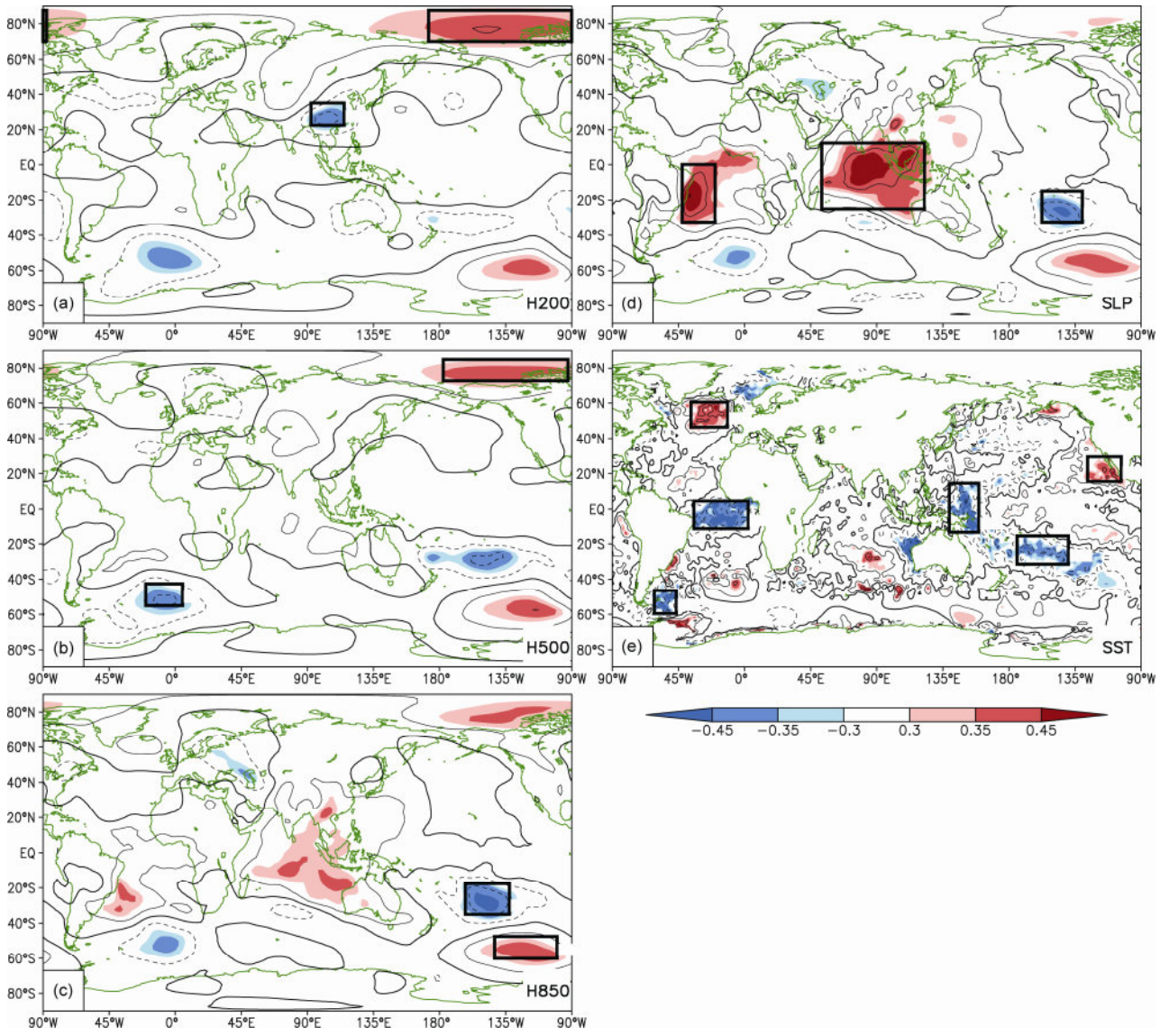


**Figure 4** Same as Figure 3 but for results after removing the signal of SNAO.

over the northern part of North America. These factors have the signals that are different from SNAO and may also influence the late-winter rainfall in SWC.

The significant correlated regions in Figure 4 are defined as the new 15 potential forcing factors. The SST factor located over the tropical Western Pacific Ocean (139.5°E–159.5°E, 13.5°S–14.5°N) has the minimum RMSE (10.6 mm) and the correlation coefficient (–0.50) is significant at the 95% confident level (Table 1). So this factor is selected and named as WPT (Western Pacific sea surface temperature). The correlation coefficient between WPT and SNAO is –0.18, implying the independence between the two factors.

In the next step, the signals of SNAO and WPT are linearly removed from SWRI according partial-correlation method:

$$\begin{aligned} \mathrm{SWRI}_2 &= \mathrm{SWRI} - \mathrm{SWRI}_{\mathrm{SNAO\_WPT}} \\ &= \mathrm{SWRI} + 3079.1 - 3.87 \times \mathrm{SNAO} + 28.5 \times \mathrm{WPT}, \end{aligned}$$

the unit of $\mathrm{SWRI}_2$, SWRI, and $\mathrm{SWRI}_{\mathrm{SNAO\_WPT}}$ is mm, and the units of SNAO and WPT are hPa and °C respectively. Figure 5 is the correlation analysis between $\mathrm{SWRI}_2$ and circulation fields. After removing the SNAO and WPT signals, some factors disappear and some reappear. The factor with the minimum RMSE is the one in the 200 hPa geopotential field over the northern Pacific (62.5°E–80°W, 52.5°N–87.5°N). But the correlation coefficient between this factor and SWRI is only 0.15, not significant at the level of 95% (Table 1), so this factor cannot be selected in the model. Besides, the other potential factors cannot pass the significant test, either, implying that after removing the signals of SNAO and WPT, the rainfall variance shows a low relationship with the large scale circulation and mainly reflects the internal variability of local rainfall. So the factor selection is over. SNAO and WPT are the selected factors related with the late-winter rainfall over SWC.

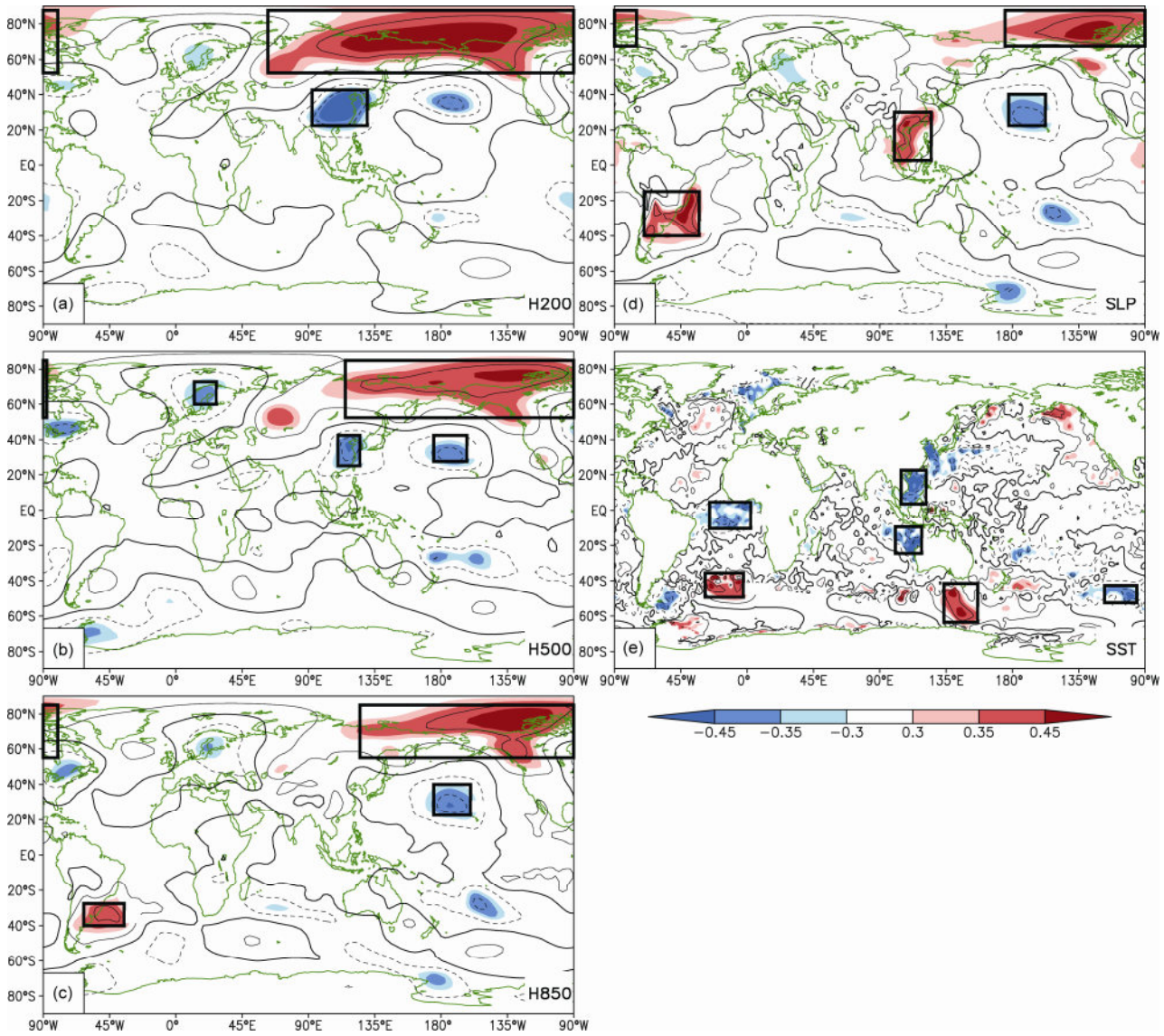


**Figure 5** Same as Figure 3 but for results after removing the signals of SNAO and WPT.

## 3 Mechanism for the influence of factors on SWRI

Two factors, SNAO and WPT, are selected using the partial-correlation method. But how the two factors affect the late-winter rainfall over SWC is still not clear. This section explains the mechanism for the influence of factors on SWRI.

### 3.1 Mechanism for the influence of SNAO on SWRI

Figure 6(a) and bare the detrended correlation analysis between SNAO and geopotential height and wind to show the circulation structure of SNAO. The geopotential height fields on all levels indicate a positive phase of winter NAO over the mid-high latitude region of North Atlantic (Li and Wang, 2003a). One negitive center is located over Greenland and the other positive center is located over western Europe and the mid lattitude of the North Atlantic. The SNAO index also shows a high correlation with the NAO and NAO indices (Table 2). These results imply that SNAO represents the variability of the southern pole of NAO.

Previous studies show that the spring NAO can excite downstream development of subpolar teleconnections across the northern Eurasia and strengthen (or weaken) the East Asian summer monsoon (Wu et al., 2009, 2012). So how does the southern pole of late-winter NAO influence the downstream rainfall over SWC? In the middle and upper troposphere in Figure 6(a) and (b), the circulation pattern shows the teleconnection response from the mid-high latitude areas of North Atlantic to the downstream regions. Three positive response centers are located in the western Europe, Arabian Sea, and the Mongolia-Northeast China region respectively, and the Red Sea and SWC show a negative response. This circulation structure is consistent with

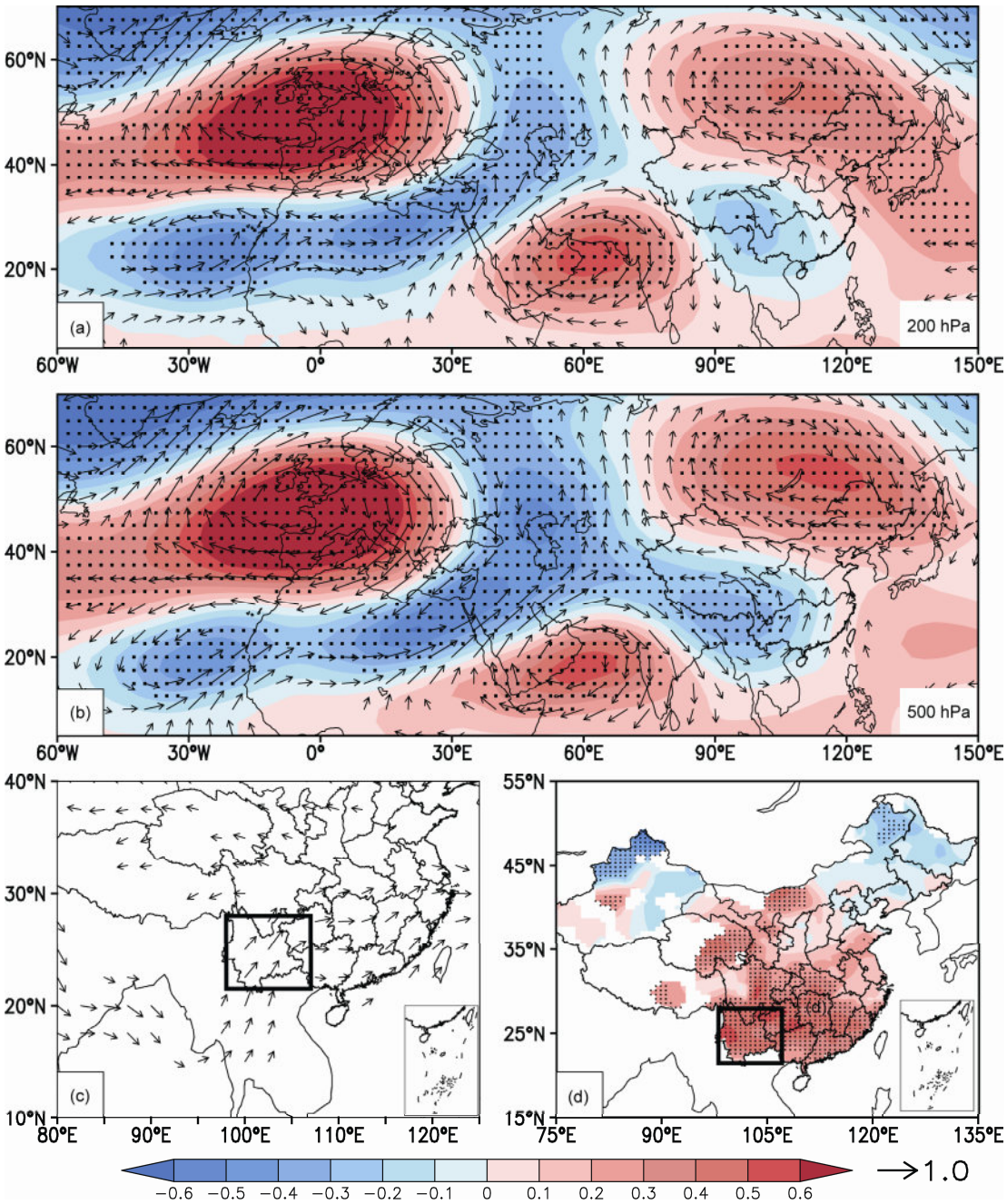


**Figure 6** Correlation pattern (detrended) between late winter SNAO and 200 hPa geopotential height and wind (a), 500 hPa geopotential height and wind (b), all level water vapor transport (c) and China rainfall (d). Stippled areas and superimposed vectors indicate statistically significant correlation at the 95% confidence level. The box indicates Southwest China region used in this study (97.5°E–107.5°E, 21.5°N–27.5°N).

the Southern Eurasian teleconnection pattern (Song et al., 2011; Xu et al., 2012). This teleconnction pattern induces a negative anomaly of geopotential height over the southern part of Tibetan Plateau, which strenghthens the southern branch trough. The southern branch trough is the main weather system over SWC. It can strengthen or weaken the southwesterly winds in the frontal trought and the water vapor transport to influcence the rainfall over SWC (Qin et al., 1991; Suo and Ding, 2009; Guo et al., 2010; Wang and Li, 2010). Figure 6(c) is the detrended correlation between SNAO and all level water vapor transport. The resutlt shows that when SNAO is positive, more water vapor from the Bay of Bengai is transported to SWC, Central and South China and enhances the late-winter rainfall over these regions.

Figure 6(d) is the detrended correlation between SNAO and late-winter rainfall over 160 gauge stations. The significant correlated regions include not only SWC but also Central and South China. This result is consistent with the forcing effect of SNAO. Besides, there is a weak negative correlated region over the northeast China, which is related

to the positive anomaly and anticyclone response over Mongolia and the Northeast China in Figure 6(a) and (b).

### 3.2 Mechanism for the influence of WPT on SWRI

Figure 7(a) is the detrended correlation between WPT and SST. The correlation pattern shows a La Niña-like structure over the tropical Pacific Ocean. There is negative correlated SST over the middle and eastern tropical Pacific, and a classic horseshoe positive pattern covers the western and subtropical Pacific. The South China Sea, northwest Pacific Ocean and the eastern Indian Ocean are negative correlated with WPT. WPT also shows negative correlation coefficients with the ENSO-related indices (Table 2). This implies that WPT represents the variability of ENSO over the tropical Western Pacific Ocean.

Tropical atmosphere circulation mainly responds to the forcing of SST anomaly (Webster, 1972; Feng et al., 2011, 2013a, 2013b). WPT represents the signal of ENSO over the Western Pacific, so the atmosphere response of WPT is similar to that of ENSO events. Figure 7(b) is the detrended correlation between WPT and 925 hPa stream function and wind. The result shows that in the positive WPT phase, there is an anticyclone structure over the north of middle

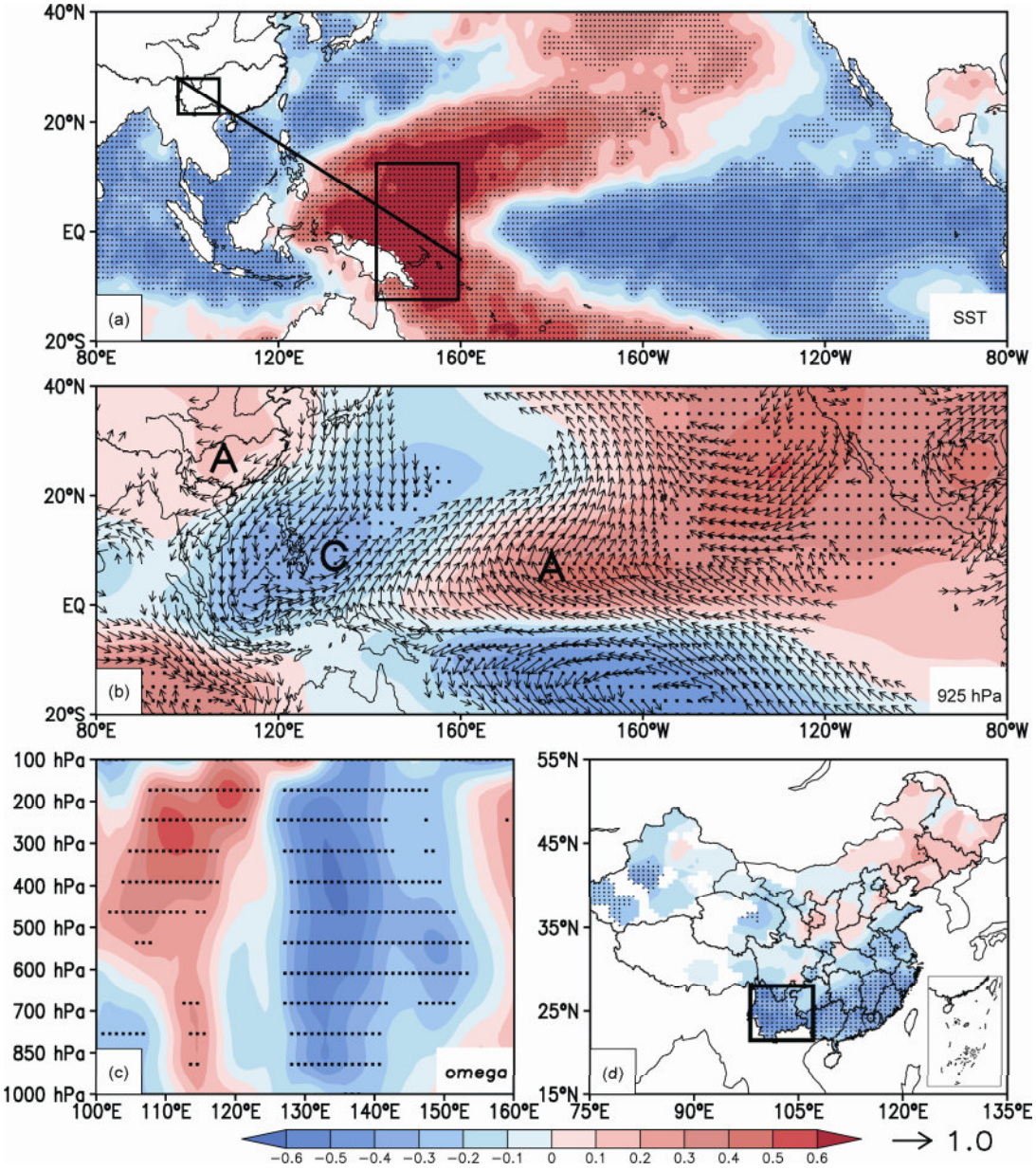


**Figure 7** Correlation pattern (detrended) between late winter WPT and (a) SST, (b) 925 hPa stream function (shaded) and 925 hPa wind (vectors), (c) omega (the cross section along the thick solid line in (a)) and (d) China rainfall. The boxes in (a) and (d) indicate the Southwest China region and WPT region. Markers A and C in (b) denote anomalous anticyclone and cyclone respectively. Stippledareas and superimposed vectors indicate statistically significant correlation at the 95% confidence level.

**Table 2** Detrended correlation coefficients between SNAO, WPT and climate indices in the late winters (1951–2014) [a)]

| | SNAO | WPT | NAO | NAM | Niño1+2 | Niño3 | Niño4 | Niño3.4 |
|---|---|---|---|---|---|---|---|---|
| SNAO | – | –0.18 | 0.74** | 0.68** | 0.17 | 0.08 | –0.04 | 0.06 |
| WPT | –0.18 | – | 0.08 | –0.04 | –0.47** | –0.53** | –0.48** | –0.56** |

a) ** Significant at the 99% level.

Pacific, which is the Rossby response of tropical atmosphere to the cold SST anomaly over the middle-east Pacific (Gill, 1980). To the west of the anticyclone, a cyclone structure is formed over the Philippine Sea and the southern China is covered by an anticyclone structure. The "A, C, A" atmosphere response is similar to the Pacific-East Asia teleconnection, which is the result of air-sea interaction over the tropical Western Pacific (Zhang et al., 1999, 2002; Wang et al., 2000; Weng et al., 2009). That is: the warm SST anomaly over the tropical western Pacific can induce cyclone response of atmosphere over the Philippine Sea. To the southeast of the anticyclone, the southwest anomaly wind is formed and overlaid to the northeast trade winds (basic states). So the total wind speed and evaporation are weakened, which favors the positive SST anomaly over tropical western Pacific and forms a positive feedback (Wang et al., 2000). Under the forcing effect of the Pacific-East Asia teleconnection, SWC is covered by the anticyclone system. The cross section of omega along (97.5°E, 27.5°N) and (160°E, 5°S) shows that there are updrafts over the Philippine Sea and downdrafts over SWC (Figure 7(c)), which will suppress the rainfall over SWC. Moreover, South China is also covered by the anticyclone and shows negative correlated rainfall with WPT.

Figure 7(d) is the detrended correlation between WPT and late-winter rainfall over 160 gauge stations. Besides SWC, the southeast coast of China also shows a significant negative correlation. The whole significant correlated regions exhibit a northeast-southwest pattern, consistent with the anticyclone forcing over the southern China.

The diagnostic analyses of circulation structures related to SNAO and WPT explain how the two forcing factors influence the late-winter rainfall over SWC. SNAO is related to the southern pole of North Atlantic Oscillation (NAO) and excites Southern Eurasian teleconnection, which influences the development of the southern branch trough and the water vapor transport to SWC. WPT indicates the variability of ENSO in the tropical Western Pacific. WPT excites Pacific-East Asia teleconnection and an anticyclone (cyclone) is formed in the southern part of China and suppresses (enhances) rainfall in SWC. It is noted that the affected areas are not confined to SWC. The southern China is also influenced by SNAO and WPT

## 4 Building and validating the model of SWRI

This section uses the forcing factors, SNAO and WPT, to build the statistical downscaling of SWRI. SWRI is the seasonal mean rainfall and the nonlinear character is weak, so linear regression model is valid. The time series of SNAO and WPT are shown in Figure 8(a). Between 1951 and 2014, the values of SNAO have not changed much but WPT exhibits an increasing trend. The increasing temperature over the tropical Western Pacific may be related to the global warming. Based on the data from 1951 to 1980, the statistical model between SNAO and WPT and late-winter SWRI is built as follows:

$$\mathrm{SWRI} = -3079.1 + 3.87 \times \mathrm{SNAO} - 28.5 \times \mathrm{WPT},$$

the units of SWRI, SNAO, and WPT are mm, hPa and °C, respectively. The estimated SWRI during 1951–1980 and 1981–2014 are calculated respectively and compared with the observed values. The results are shown in Figure 8(b) and Table 3. During the model training period, the correlation coefficient between the observed and estimated SWRI is 0.79 and the RMSE of cross validation is 10.8 mm, and the anomaly sign consistency rate is 83%. The regression model shows good performance in simulating the change of SWRI. During the independent validation period, the correlation coefficient, RMSE, and the anomaly sign consistency rate are 0.79, 9.9 mm, and 71%, respectively. So the statistical model shows a similar skill in training and validating periods, which implies the robustness and reliability of the model.

When the severe drought occurred in the winter of 2009/2010, the SNAO was in the strong negative phase while the anomaly of WPT was weak (Figure 8(a)). The estimated rainfall is 9.74 mm, similar to the observation (10.1 mm). This result implies that the 2009/2010 drought was caused by the extreme forcing from the mid-high latitude regions and was weakly related with tropical SST. This conclusion is consistent with parts of previous studies (Song et al., 2011; Xu et al., 2012; Yang et al., 2012). But the model in this paper is based on the linear analysis. Some studies have shown that the nonlinear influence of ENSO on the autumn rainfall over the southern China causes the decadal drough in this region (Zhang et al., 2011, 2014). So, further research is needed to check whether tropical SST also has a nonlinear effect on late-winter rainfall over SWC.

SWRI is the regional average rainfall over the whole Southwest China. Then we study the statistical model performance on every station rainfall. We still take SNAO and WPT as the forcing factors and take the observed station rainfall as the predictand. A binary linear regression model is built for each station and tested during 1981–2014. The

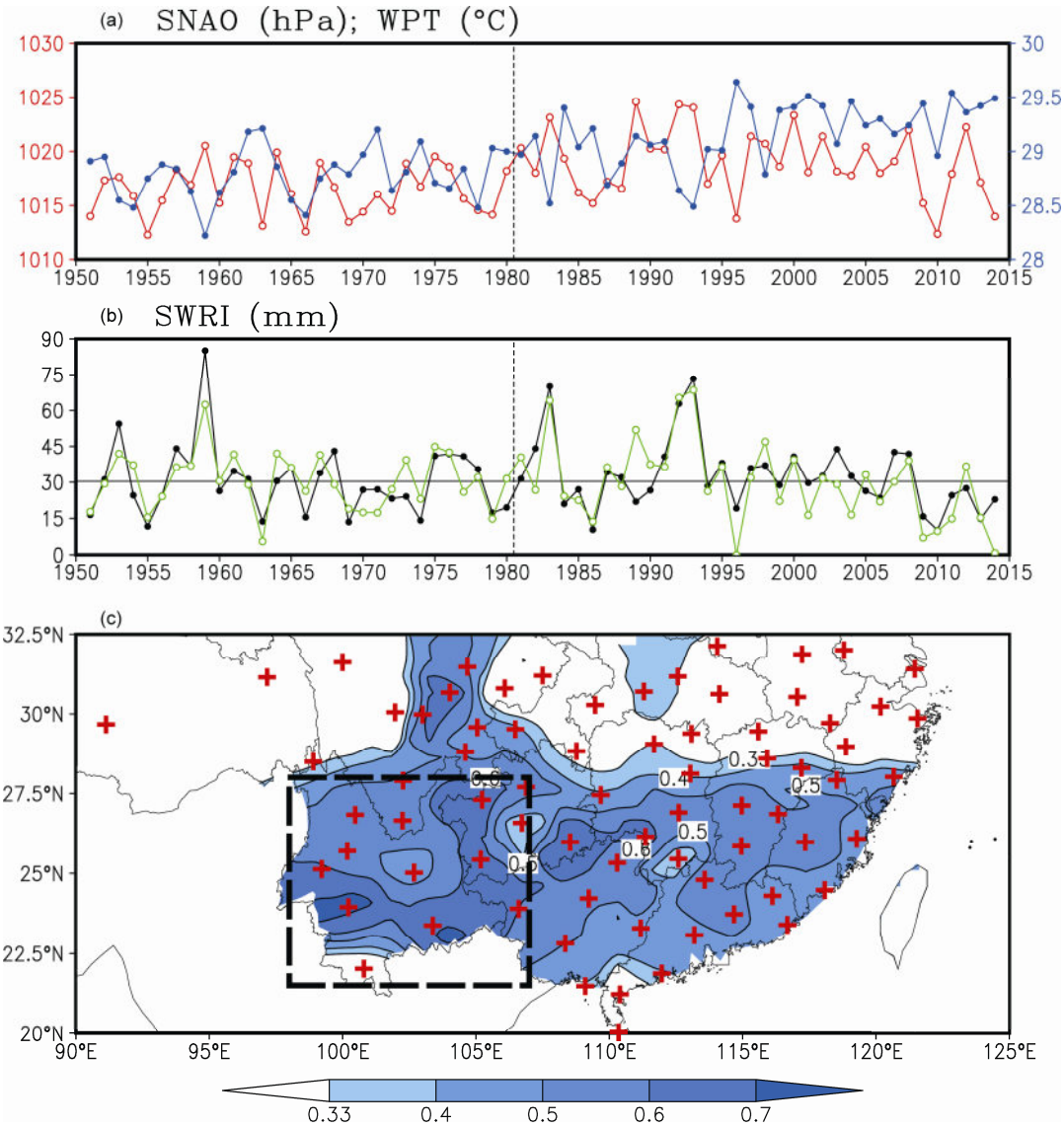


**Figure 8** Time series of late winter SNAO and WPT (a) and observed and fitted SWRI (b), correlation pattern between observed and fitted late winter rainfall for each observation station during 1981–2014 (c). The training period in (b) is 1951–1980 and the independent validation period is 1981–2014; the straight line is the long-term mean (1951–2014). The shaded areas in (c) indicate statistically significant correlation at the 95% confidence level. The dashed box indicates Southwest China region used in this study (97.5°E–107.5°E, 21.5°N–27.5°N). The red crosses indicate the distribution of 160 gauge stations.

**Table 3** Correlation coefficients, RMSE in cross validation and anomaly sign consistency rate between observed and fitted late-winter SWRI during the training period (1951–1980) and the independent validation period (1981–2014)

| | Cor. | RMSE (mm) | *P* |
|---|---|---|---|
| Training period (1951–1980) | 0.79 | 10.8 | 83% |
| Validation period (1981–2014) | 0.79 | 9.9 | 71% |

correlation coefficients are shown in Figure 8(c). The result shows that the statistical model performs well for the whole SWC region except for the southernmost station of Hongjing. The correlation coefficients are more than 0.50 in most stations and exceeding 0.70 in some stations. The result shows that the statistical model with SNAO and WPT is also valid for the station rainfall over SWC. Besides, the model exhibits some skill in South China although the model is originally designed for the SWC region, which is the result of the SNAO and WPT influences on the rainfall over the southern China.

## 5 Discussion and summary

SWC suffered consecutive droughts in recent decades, and the continuous drought from the autumn of 2009 to the winter of 2010 was the most severe event since the records began. This paper analyzes the attribution of the late-winter

rainfall over SWC and proposes partial-correlation method to build the statistical downscaling model. The two selected factors are SNAO over the western Europe and WPT over the western tropical Pacific. The statistical model with the two factors shows good performance in estimating the rainfall over the whole SWC region and every observation station. The model also shows robustness and reliability in the independent validation.

Both SNAO and WPT influence the late-winter rainfall over SWC through teleconnections. SNAO shows the variability of the southern NAO pole and induces Southern Eurasian teleconnection in the winter. The excited Rossby waves propagate by the way of the western Europe, the Red Sea, the Arabic Sea, and the southern part of Tibet Plateau. The teleconnection influences the strength of the southern branch trough and water vapor transport, which further influence the rainfall over SWC. WPT reflects the effect of ENSO on SWRI. In the positive phase of WPT, the La Niña-like pattern of SST in the tropical Pacific excites Pacific-East Asian Teleconnection, which induces the A-C-A response of atmosphere along the Philippine Sea and the southern China. SWC is covered by anticyclone and down-drafts suppress the rainfall.

SNAO and WPT show the influence of NAO and ENSO on the late-winter rainfall over SWC, so is it valid to build the model with NAO and ENSO? A new regression model with the NAO and Niño3.4 indices is built and validated to evaluate the model's performance. The result shows that the estimation skill of the new model is worse than the model with SNAO and WPT. The correlation coefficient, RMSE, and the anomaly sign consistency rate are 0.59, 12.69 mm, and 68%, respectively. The possible reason is that NAO and ENSO influence SWRI through SNAO and WPT, so the direct relationship between NAO and ENSO and SWRI is weaker. Besides, other studies found that the forcing effect of ENSO is nonlinear (Zhang et al., 2011, 2014), which is another possible reason for the poor performance of NAO and Niño3.4 in a linear model.

Both the forcing factors and predictand in this paper are in the late winter, so the statistical model cannot make prediction alone. Numeric models are needed in the practical prediction. Are there any preceding forcing factors related to SWRI and how to build a preceding statistical downscaling model? Besides, we found that the model in this paper also shows good skill in estimating the rainfall over South China. What is the relationship of interannual and interdecadal variability between SWC and South China? How to build the model for South China? These questions are still not clear and further work is needed in the future.

*This work was jointly supported by the "Strategic Priority Research Program - Climate Change: Carbon Budget and Relevant Issues" of the Chinese Academy of Sciences (Grant No. XDA05090403), the National Key Program for Developing Basic Sciences (Grant No. 2013CB430200) and the National Natural Science Foundation of China (Grant No. 41205046).*

Barriopedro D, Gouveia C M, Trigo R M, et al. 2012. The 2009/10 drought in China: Possible causes and impacts on vegetation. J Hydrometeor, 13: 1251–1267

Feng J, Li J P. 2013a. Contrasting impacts of two types of ENSO on the boreal spring Hadley circulation. J Clim, 26: 4773–4789

Feng J, Li J P, Xie F. 2013b. Long-term variation of the principal mode of boreal spring Hadley circulation linked to SST over the Indo-Pacific warm pool. J Clim, 26: 532–544

Feng L, Li T, Yu W. 2014. Cause of severe droughts in Southwest China during 1951–2010. Clim Dyn, 43: 2033–2042

Feng R, Li J P, Wang J C. 2011. Regime change of the boreal summer Hadley circulation and its connection with the tropical SST. J Clim, 24: 3867–3877

Fowler H, Blenkinsop S, Tebaldi C. 2007. Linking climate change modelling to impacts studies: Recent advances in downscaling techniques for hydrological modelling. Int J Climatol, 27: 1547–1578

Gill A E. 1980. Some simple solutions for heat-induced tropical circulation. Q J R Meteorol Soc, 106: 447–462

Gu W, Wang L, Li W, et al. 2014. Influence of the tropical Pacific east-west thermal contrast on the autumn precipitation in South China. Int J Climatol, doi: 10.1002/joc.4075

Guo R, Gao A, Yang S. 2010. Comparison analysis of two heavy rain processes on the plateau at low lattitude caused by the southern branch trough in winter (in Chinese). Trans Atmos Sci, 33: 82–88

Guo Y, Li J P, Li Y. 2011. Statistically downscaled summer rainfall over the middle-lower reaches of the Yangtze River. Atmos Oceanic Sci Lett, 4: 191–198

Guo Y, Li J P, Li Y. 2012. A time-scale decomposition approach to statistically downscale summer rainfall over North China. J Clim, 25: 572–591

Guo Y, Li J P, Li Y. 2014. Seasonal forecasting of North China summer rainfall using a statistical downscaling model. J Appl Meteor Climatol, 53: 1739–1749

Hewitson B, Crane R. 2006. Consensus between GCM climate change projections with empirical downscaling: precipitation downscaling over South Africa. Int J Climatol, 26: 1315–1337

Huang R, Liu Y, Wang L, et al. 2012. Analyses of the cause of severe drought occuring in Southwest China from the fall of 2009 to the spring of 2010 (in Chinese). Chin J Atmos Sci, 36: 443–457

Kalnay E, Kanamitsu M, Kistler R, et al. 1996. The NCEP/NCAR 40-year reanalysis project. Bull Amer Meteorol Soc, 77: 437–471

Li J P, Wang J X. 2003a. A new North Atlantic Oscillation index and its variability. Adv Atmos Sci, 20: 661–676

Li J P, Wang J X. 2003b. A modified zonal index and its physical sense. Geophys Res Lett, 30: 1632

Li J P, Rong R, Qi Y, et al. 2013a. Progress in air-land-sea interactions in Asia and their role in global and Asian climate change (in Chinese). Chin J Atmos Sci, 37: 518–538

Li, J P, Sun C, Jin F F. 2013b. NAO implicated as a predictor of Northern Hemisphere mean temperature multidecadal variability. Geophys Res Lett, 40: 5497–5502

Li Y, Smith I. 2009. A statistical downscaling model for southern Australia winter rainfall. J Clim, 22: 1142–1158

Liu J, Tan X, Wan J, et al. 2011. Comparative analysis between the 2010 severe drought in southwest Chian and typical drought disasters (in Chinese). Chin Water Resour, 9: 17–19

Qin J, Pan L, Shi L. 1991. The influence of the southern branch trough and the cold air on the winter weather in Yunnan (in Chinese). Meteor Mon, 17: 39–43

Rayner N A, Parker D E, Horton E B, et al. 2003. Global analyses of sea surface temperature, sea ice, and night marine air temperature since the late nineteenth century. J Geophys Res: Atmos, 108: 4403

Salathé E P. 2003. Comparison of various precipitation downscaling methods for the simulation of streamflow in a rainshadow river basin. Int J Climatol, 23: 887–901

Song J, Yang H, Li C. 2011. A further study of causes of the severe drought in Yunnan Province during the 2009/2010 winter (in Chinese). Chin J Atmos Sci, 35: 1009–1019

Suo M, Ding Y. 2009. The structures and evolutions of the wintertime southern branch trough in the subtropical westerlies (in Chinese). Chin J Atmos Sci, 33: 425–442

Tao Y, Huang W, Zheng J, et al. 2014. Evolutive features and its causes of the wintertime precipitation in Yunnan Province (in Chinese). Plateau Meteor, 33: 130–139

Wang B, Li Y. 2010. Relationship analysis between south branch trough and severe drought of southwest China during autumn and winter 2009/2010 (in Chinese). Plateau Mountain Meteor Res, 30: 26–35

Wang B, Wu R, Fu X. 2000. Pacific-East Asian teleconnection: How does ENSO affect East Asian climate? J Clim, 13: 1517–1536

Wang L, Chen W, Zhou W. 2014. Assessment of future drought in Southwest China based on CMIP5 multimodel projections. Adv Atmos Sci, 31: 1035–1050

Webster P J. 1972. Response of the tropical atmosphere to local, steady forcing. Mon Weather Rev, 100: 518–541

Weng H, Behera S K, Yamagata T. 2009. Anomalous winter climate conditions in the Pacific rim during recent El Niño Modoki and El Niño events. Clim Dyn, 32: 663–674

Wilby R L. 1997. Non-stationarity in daily precipitation series: Implications for GCM downscaling using atmospheric circulation indices. Int J Climatol, 17: 439–454

Wilby R L, Wigley T. 2000. Precipitation predictors for downscaling: Observed and general circulation model relationships. Int J Climatol, 20: 641–661

Wu Z, Wang B, Li J P, et al. 2009. An empirical seasonal prediction model of the East Asian summer monsoon using ENSO and NAO. J Geophys Res, 114: D18120

Wu Z, Li J P, Jiang Z, et al. 2012. Possible effects of the North Atlantic Oscillation on the strengthening relationship between the East Asian summer monsoon and ENSO. Int J Climatol, 32: 794–800

Xu H, Li J P, Feng J, et al. 2012. The asymmetric relationship between the winter NAO and the precipitation in Southwest China (in Chinese). Acta Meteorol Sin, 70: 1276–1291

Yarnal B, Comrie A C, Frakes B, et al. 2001. Developments and prospects in synoptic climatology. Int J Climatol, 21: 1923–1950

Yang H, Song J, Yan H, et al. 2012. Cause of the severe drought in Yunnan Province during winter of 2009 to 2010 (in Chinese). Chin J Atmos Sci, 17: 315–326

Yu M, Li Q, Hayes M J, et al. 2014. Are droughts becoming more frequent or severe in China based on the standardized precipitation evapotranspiration index: 1951–2010? Int J Climatol, 34: 545–558

Zhang L, Xiao J, Li J, et al. 2012. The 2010 spring drought reduced primary productivity in southwestern China. Environ Res Lett, 7: 045706

Zhang M, He J, Wang B, et al. 2013a. Extreme drought changes in Southwest China from 1960 to 2009. J Geogr Sci, 23: 3–16

Zhang R, Sumi A. 2002. Moisture circulation over East Asia during El Niño episode in northern winter, spring and autumn. J Meteorol Soc Jpn, 80: 213–227

Zhang R, Sumi A, Kimoto M. 1999. A diagnostic study of the impact of El Nino on the precipitation in China. Adv Atmos Sci, 16: 229–241

Zhang W, Jin F F, Li J P, et al. 2011. Contrasting impacts of two-type El Nino over the Western North Pacific during boreal autumn. J Meteorol Soc Jpn, 89: 563–569

Zhang W, Jin F F, Zhao J X, et al. 2013b. The possible influence of a non-conventional El Niño on the severe autumn drought of 2009 in Southwest China. J Clim, 26: 8392–8405

Zhang W, Jin F F, Turner A. 2014. Increasing autumn drought over southern China associated with ENSO regime shift. Geophys Res Lett, 41: 4020–4026

Zhang W, Wang L, Xiang B, et al. 2015. Impacts of two types of La Nina on the NAO during boreal winter. Clim Dyn, 44: 1351–1366

Zorita E, Storch H V. 1999. The analog method as a simple statistical downscaling technique: Comparison with more complicated methods. J Clim, 12: 2474–2489